European Congress on Computational Methods in Applied Sciences and Engineering
ECCOMAS 2000
Barcelona, 11-14 September 2000

SIMULATION OF MAGNETOHYDRODYNAMICS WITH HEAT TRANSFER

Brian H. Dennis[*] and George S. Dulikravich[†]

[*]Department of Aerospace Engineering, 233 Hammond,
The Pennsylvania State University,
University Park, PA 16802, U.S.A
E-mail address: bhd102@psu.edu

[†]Department of Mechanical and Aerospace Engineering, Box 19018,
The University of Texas at Arlington,
Arlington, TX 76019, U.S.A
E-mail address: gsd@uta.edu

Key words: Magnetohydrodynamics, least-squares finite element method, conjugate heat transfer

Abstract. *In this paper we consider the problem of multidisciplinary analysis of steady, incompressible magnetohydrodynamic (MHD) flow with conjugate heat transfer in 2-D. A computer program was developed based on the least-squares finite element method to simulate MHD flows with conjugate heat transfer. Numerical simulations will be shown that demonstrate the effect of applied magnetic fields on an incompressible, electrically conducting fluid. The effect on the heat transfer between that fluid and a solid wall will also be shown.*

1 Introduction

In this paper we consider the problem of multidisciplinary analysis of steady, incompressible magnetohydrodynamic (MHD) flow with conjugate heat transfer. Numerical simulations will be shown that demonstrate the affect of applied magnetic fields on an incompressible, electrically conducting fluid in 2-D. The affect on the heat transfer between that fluid and a solid wall will also be shown.

Simulations of steady, incompressible, 2-D and 3-D MHD flows were demonstrated in [1, 2]. The authors showed the effect of applied magnetic fields on the flow field and temperature field. In both cases the authors used a finite difference based method with structured grids and did not consider the conjugate heat transfer.

The simulation code used for MHD simulations presented here is based on a variant of finite element method commonly know as the least-squares finite element method (LSFEM). The least-squares finite element method has been applied successfully to many problems, including steady and unsteady incompressible 2-D flows [3, 4]. There are several advantages to using LSFEM. First, the LSFEM produces symmetric positive definite systems of algebraic equations that can be solved efficiently by simple iterative methods such as the preconditioned conjugate gradient method. Furthermore, the LSFEM can be applied to equations or systems of equations of any type without any special treatment which makes it an ideal method for use in multidisciplinary problems involving various kinds of physics, such as MHD. Another benefit of using LSFEM is that it is not subject to the restrictive *inf-sup* condition [3]. Equal order approximation functions can be employed for all unknowns without causing instability.

2 Simulation of MHD Flows

A magnetohydrodynamic flow can be described as the flow of an electrically conducting incompressible fluid through an applied magnetic field. The following sections give an overview of the equations governing MHD flows with heat transfer as well as the LSFEM numerical method that is used for numerical simulation of such flows.

2.1 Governing Equations

The steady viscous incompressible MHD flow can be described by the Navier-Stokes equations combined with the Maxwell's equations.

$$\nabla \cdot \mathbf{V} = 0 \tag{1}$$

$$\rho \mathbf{V} \cdot \nabla \mathbf{V} - \eta \nabla^2 \mathbf{V} + \nabla P - \sigma \mathbf{V} \times \mathbf{B} \times \mathbf{B} = 0 \tag{2}$$

$$\rho C_p \mathbf{V} \cdot \nabla T - \nabla \cdot (k \nabla T) - \frac{1}{\sigma} \mathbf{J} \cdot \mathbf{J} = 0 \tag{3}$$

$$\nabla \cdot \mathbf{B} = 0 \tag{4}$$

$$\nabla \times \mathbf{B} = \mu \mathbf{J} \tag{5}$$

$$\mathbf{J} = \sigma \mathbf{V} \times \mathbf{B} \tag{6}$$

(7)

Here, $\mathbf{V}$ is the fluid velocity, ρ is the fluid density, Cp is the specific heat, P is the hydrodynamic pressure, k is the heat conductivity coefficient, η is the coefficient of viscosity, $\mathbf{B}$ is the magnetic flux density, μ is the magnetic permeability coefficient, $\mathbf{J}$ is the current density, and σ is the electrical conductivity of the fluid. Only the presence of a steady magnetic field is considered here so the equations and terms in Maxwell's equations relating to the electric field are omitted. Simulations of fluid flow with applied magnetic and electric fields would require a much more complicated mathematical model [5].

For computations, we use the corresponding non-dimensional form of the above equations

$$\nabla^* \cdot \mathbf{V}^* = 0 \tag{8}$$

$$\mathbf{V}^* \cdot \nabla^* \mathbf{V}^* - \tfrac{1}{Re}\nabla^{*2}\mathbf{V}^* + \nabla^* P^* - \tfrac{Ht^2}{Re}\mathbf{V}^* \times \mathbf{B}^* \times \mathbf{B}^* = 0 \tag{9}$$

$$\mathbf{V}^* \cdot \nabla T^* - \tfrac{1}{Pe}\nabla^{*2}T^* - \tfrac{Ht^2 Ec}{Re}(\mathbf{V}^* \times \mathbf{B}^*)^2 = 0 \tag{10}$$

$$\nabla^* \cdot \mathbf{B}^* = 0 \tag{11}$$

$$\nabla^* \times \mathbf{B}^* = Rm\mathbf{V}^* \times \mathbf{B}^* \tag{12}$$

where $V^* = V\,U_0^{-1}$, $B^* = B\,B_0^{-1}$, $P^* = P\,\rho^{-1}U_0^{-2}$, $x^* = x\,L_0^{-1}$, $y^* = y\,L_0^{-1}$, $T^* = \frac{T - T_{cold}}{\Delta T_0}$. Here, L_0 is the reference length, U_0 is the reference speed, and B_0 is the reference magnetic flux density. The temperature is nondimensionalized with a temperature difference, ΔT, where $\Delta T = T_{hot} - T_{cold}$. For convenience the $*$ superscript will be dropped for the remainder of the paper.

The nondimensional numbers are given by:

Reynolds number	Re	$= \dfrac{\rho U_0 L_0}{\eta}$
Magnetic Reynolds number	Rm	$= \mu\sigma U_0 L_0$
Hartmann number	Ht	$= L_0 B_0 \sqrt{\dfrac{\sigma}{\eta}}$
Peclet number	Pe	$= \dfrac{L_0 u_0 \rho Cp}{k}$
Eckert number	Ec	$= \dfrac{u_0^2}{Cp\Delta T}$

2.2 Least-Squares Finite Element Method

The system of partial differential equations described in section 2.1 is discretized using the least squares finite element method. We first look at the LSFEM for a general linear first-order system.

$$[L]\mathbf{u} = \mathbf{f} \tag{13}$$

where

$$[L] = [A_1]\frac{\partial}{\partial x} + [A_2]\frac{\partial}{\partial y} + [A_3] \tag{14}$$

The residual of the system is represented by $\mathbf{R}$.

$$\mathbf{R}(\mathbf{u}) = [L]\mathbf{u} - \mathbf{f} \tag{15}$$

We now define the following least squares functional I over the domain Ω

$$I(\mathbf{u}) = \int_\Omega \mathbf{R}(\mathbf{u})^T \cdot \mathbf{R}(\mathbf{u})\, dx\, dy \tag{16}$$

The weak statement is then obtained by taking the variation of I with respect to $\mathbf{u}$ and setting the result equal to zero.

$$\delta I(\mathbf{u}) = \int_\Omega ([L]\delta\mathbf{u})([L]\mathbf{u} - \mathbf{f})\, dx\, dy = 0 \tag{17}$$

Using equal order shape functions, ϕ_i, for all unknowns, the vector $\mathbf{u}$ is written as

$$\mathbf{u} = \sum_{i=1}^{n} \phi_i \{u_1, u_2, u_3, ..., u_m\}_i^T \tag{18}$$

where $\{u_1, u_2, u_3, ..., u_m\}_i$ are the nodal values at the ith node of the finite element. Introducing the above approximation for $\mathbf{u}$ into the weak statement leads to a linear system of algebraic equations

$$[K]\mathbf{U} = \mathbf{F} \tag{19}$$

where $[K]$ is the stiffness matrix, $\mathbf{U}$ is the vector of unknowns, and $\mathbf{F}$ is the force vector.

2.3 LSFEM for Magnetohydrodynamics

Use of LSFEM for systems of equations that contain higher order derivatives is usually difficult due to the higher continuity restrictions imposed on the approximation functions. For this reason, it is more convenient to transform the system into an equivalent first order form before applying LSFEM. For the case of magnetohydrodynamics, the second order derivatives are transformed by introducing vorticity, ω, as an additional unknown. The energy equation is also transformed into first order form by introducing fluxes as additional unknowns.

$$\nabla \cdot \mathbf{V} = 0 \tag{20}$$

$$\mathbf{V} \cdot \nabla\mathbf{V} + \tfrac{1}{Re}\nabla \times \omega + \nabla P - \tfrac{Ht^2}{Re}\mathbf{V} \times \mathbf{B} \times \mathbf{B} = 0 \tag{21}$$

$$\omega - \nabla \times \mathbf{V} = 0 \tag{22}$$

$$\mathbf{V} \cdot \nabla T + \nabla \cdot \mathbf{q} - \tfrac{Ht^2 Ec}{Re}(\mathbf{V} \times \mathbf{B})^2 = 0 \tag{23}$$

$$\mathbf{q} + \tfrac{1}{Pe}\nabla T = 0 \tag{24}$$

$$\nabla \times \mathbf{q} = 0 \tag{25}$$

$$\nabla \cdot \mathbf{B} = 0 \tag{26}$$

$$\nabla \times \mathbf{B} = Rm\mathbf{V} \times \mathbf{B} \tag{27}$$

It should be noted that a curl free condition on the flux vector field appears in the first-order form of energy equation. It was shown in [6] that the presence of this condition is required for achieving optimal convergence rates for the flux vector, $\mathbf{q}$. It was also shown in [6] that the inclusion of the curl free condition does not produce an over determined system of equations.

We consider a two-dimensional problem only and write the above system in the general form of a first-order system (13). Although the entire system written in (20)-(27) can be treated by LSFEM, it was found to be more economical to solve the fluid, heat transfer, and magnetic field equations separately, in an iterative manner. Here, a general form first order system is written for the fluid system (20)-(22) and denoted by the superscript *fluid*. A first-order system is also written in general form for the magnetic field equations (26)-(27) and is denoted by the superscript *mag*. The first-order system written in general form for the heat transfer equations (23)-(24) is denoted by the superscript *heat*. In addition, the nonlinear convective terms in the fluid equations are linearized with Newton's method leading to a system suitable for treatment with the LSFEM described in section 2.2.

$$\left[A_1^{fluid}\right] = \begin{bmatrix} 1 & 0 & 0 & 0 \\ u & 0 & 1 & 0 \\ 0 & u & 0 & -\frac{1}{Re} \\ 0 & -1 & 0 & 0 \end{bmatrix}, \qquad \left[A_2^{fluid}\right] = \begin{bmatrix} 0 & 1 & 0 & 0 \\ v & 0 & 0 & \frac{1}{Re} \\ 0 & v & 1 & 0 \\ 1 & 0 & 0 & 0 \end{bmatrix},$$

$$\left[A_3^{fluid}\right] = \begin{bmatrix} 0 & 0 & 0\,0 \\ \frac{Ht^2}{Re}B_{y0}^2 & -\frac{Ht^2}{Re}B_{x0}B_{y0} & 0\,0 \\ -\frac{Ht^2}{Re}B_{x0}B_{y0} & \frac{Ht^2}{Re}B_{x0}^2 & 0\,0 \\ 0 & 0 & 0\,1 \end{bmatrix},$$

$$\mathbf{f}^{fluid} = \left\{ \begin{matrix} 0 \\ u_0\frac{\partial u_o}{\partial x} + v_0\frac{\partial u_o}{\partial y} \\ u_0\frac{\partial v_o}{\partial x} + v_0\frac{\partial v_o}{\partial y} \\ 0 \end{matrix} \right\}, \qquad \mathbf{u}^{fluid} = \left\{ \begin{matrix} u \\ v \\ p \\ \omega \end{matrix} \right\} \tag{28}$$

$$[A_1^{mag}] = \begin{bmatrix} 1 & 0 \\ 0 & 1 \end{bmatrix}, [A_2^{mag}] = \begin{bmatrix} 0 & 1 \\ -1 & 0 \end{bmatrix}, [A_3^{mag}] = \begin{bmatrix} 0 & 0 \\ Rm\,v_0 & -Rm\,u_0 \end{bmatrix},$$

$$\mathbf{f}^{mag} = \left\{ \begin{matrix} 0 \\ 0 \end{matrix} \right\}, \qquad \mathbf{u}^{mag} = \left\{ \begin{matrix} B_x \\ B_y \end{matrix} \right\} \tag{29}$$

$$\left[A_1^{heat}\right] = \begin{bmatrix} u & 1 & 0 \\ \frac{1}{Pe} & 0 & 0 \\ 0 & 0 & 0 \\ 0 & 0 & -1 \end{bmatrix}, \left[A_2^{heat}\right] = \begin{bmatrix} v & 0 & 1 \\ 0 & 0 & 0 \\ \frac{1}{Pe} & 0 & 0 \\ 0 & 1 & 0 \end{bmatrix}, \left[A_3^{heat}\right] = \begin{bmatrix} 0 & 0 & 0 \\ 0 & 1 & 0 \\ 0 & 0 & 1 \\ 0 & 0 & 0 \end{bmatrix},$$

$$\mathbf{f}^{heat} = \left\{ \begin{array}{c} \frac{Ht^2 Ec}{Re}(u_0 B_{y0} - v_0 B_{x0})^2 \\ 0 \\ 0 \\ 0 \end{array} \right\}, \qquad \mathbf{u}^{heat} = \left\{ \begin{array}{c} T \\ q_x \\ q_y \end{array} \right\} \tag{30}$$

A solution satisfying all of the above systems of equations can be found by using a simple iterative process. First, the system in (28) is solved with the magnetic field given from an initial guess or from the previous iteration. Next,the system given in (29) is solved using the recently calculated velocity field. This process is repeated until a specified convergence tolerance is reached. For most cases considered in this paper, reduction of the residual norm of both systems by 3.5 orders of magnitude was achieved in less than 5 iterations. Once the velocity and magnetic fields are determined, the system in (30) is solved to obtain the temperature distribution.

2.4 Verification of Accuracy

The accuracy of the LSFEM for MHD was tested against known analytic solutions for Poisuille-Hartmann flow. The Poisuille-Hartmann flow is a 1-D flow of a conducting and viscous fluid between two stationary plates with a uniform external magnetic field applied orthogonal to the plates. Assuming the walls are at $y = \pm L$ and that fluid velocity on the walls is zero and that the fluid moves in the x-direction under the influence of a constant pressure gradient, then the velocity profile is given by [7, 8]

$$u(y) = \frac{\rho Ht}{\sigma B_y^2} \frac{\partial p}{\partial x} \left(\frac{\cosh(Ht) - \cosh(\frac{Hty}{L})}{\sinh(Ht)} \right) \tag{31}$$

The movement of the fluid induces a magnetic field in the x-direction and is given by

$$B_x(y) = \frac{B_y Rm}{Ht} \left(\frac{\sinh(\frac{Hty}{L}) - (\frac{y}{L}\sinh(Ht)}{\cosh(Ht) - 1} \right) \tag{32}$$

A test case was run using the parameters given in Table 1 and with a mesh composed of 2718 parabolic triangular elements. Figure 1 shows the computed and analytical results for the velocity profile. Figure 2 shows the computed and analytical results for the induced magnetic field. For both cases, one can see that the agreement between the analytical solution and the LSFEM solution is excellent.

3 Numerical Results

One would guess that the application of a magnetic field to a flowing electrically conducting fluid, such as seawater, would result in a noticeable change in the flow field. Also, the application of a magnetic field could alter the heat transfer characteristics of such a flow.

The flow of hot seawater through a 2-D pipe with a finite thickness solid cold wall was used to demonstrate the effect of an applied magnetic field on the flow field and the heat transfer characteristics. This example problem also shows the ability of the LSFEM to compute the approximate solutions to such a multidisciplinary problem involving a variety of different physics.

Figure 3 shows the domain of the problem. It is evident that this is a conjugate heat transfer problem involving the computation of the thermal field in both the solid and fluid region simultaneously.

The inlet height was 2 m and the channel length was 15 m. The solid plate thickness was .25 m. Table 2 shows the physical properties used for this problem. Since the domain is symmetric, only the bottom half was considered.

The MHD analysis was performed by a LSFEM code written in C/C++. A mesh of triangular parabolic elements was used [9]. A typical mesh is shown in figure 3. A parabolic velocity profile was specified at the upstream boundary while a uniform static pressure was specified at the downstream boundary. A no-slip boundary condition for velocity was specified at the fluid/solid interface. Zero normal component of the magnetic field was enforced on the fluid/solid interface except in the regions of $7.0 <= x <= 8.0$, where a sinusoidal variation in the magnetic field components was specified. The flow inlet temperature was set to 2000 K. The temperature on the bottom and left boundary of the plate was fixed at 300 K. The zero flux boundary condition was used on the outlet and right side of the plate. The symmetry boundary condition was applied to the top of domain.

The sparse linear system for the magnetic field, fluid flow, and heat transfer were solved with a sparse LU code [10] at each nonlinear iteration. All computations were made on a Pentium II 400 MHz based PC. A typical run requires around ten minutes. Convergence history for a typical analysis is shown in figure 4.

The simulation code was run for several values of Ht by varying the maximum magnetic flux, B_0, from 0.0 to 3.0 Tesla. The following non-dimensional parameters were kept fixed: $Re = 614.4$, $Pe = 5141.3$, $Rm = 2.7 \times 10^{-9}$, and $Ec = 8.6 \times 10^{-11}$. Figures 5-6 show the variation of temperature and heat flux on the fluid solid interface for various magnetic field strengths. The application of magnetic field seems to strongly affect the heat transfer, particularly in the region where the magnetic field is applied as well as further downstream. In Figures 7-8, the change in the temperature distribution when the sinusoidal magnetic field distribution is applied can be clearly seen. Figures 9-11 show that the presence of the magnetic field induces a large separation in the flow field close to the wall. The size and complexity of separation flow is proportional to the strength of the applied magnetic field.

It should also be noted that the presence of the flow field can induce changes in the steady state magnetic field. Figures 13 and 15 show the transport of the magnetic field in the convective direction. However, it was found that a relatively high value of $Rm = 20$ was required to produce a highly noticeable effect.

4 Conclusion

A MHD simulation code has been developed based on the LSFEM. It shows excellent agreement with known analytic solutions for Poisuille-Hartmann flow. The MHD simulation code was applied to a conjugate heat transfer problem of a hot flow through a duct with an applied magnetic field and a cold solid wall. The LSFEM MHD code showed the change in heat transfer characteristics with the application of various strengths of applied magnetic fields. The LSFEM MHD code also showed the complex separation bubbles created near the wall by the applied magnetic fields.

REFERENCES

[1] G. S. Dulikravich, K. Y. Choi, and S. Lee. Magnetic field control of vorticity in steady incompressible laminar flows. In D. A. Siginer, J. H. Kim, S. A. Sheriff, and H. W. Colleman, editors, *ASME WAM94 Symposium on Electrorheological Flows-II.* Chicago, IL, Nov. 6-11,1994, ASME FED-Vol. 205/AMD-Vol. 190, pp. 125-142., 1994.

[2] S. Lee and G. S. Dulikravich. Magnetohydrodynamic steady flow computations in three dimensions. *International Journal for Numerical Methods in Fluids*, 13:917–936, 1991.

[3] B.-N. Jiang. A least-squares finite element method for incompressible navier-stokes problems. *International Journal for Numerical Methods in Fluids*, 14:843–859, 1992.

[4] L. Q. Tang and T. H. Tsang. A least-squares finite element method for time-dependant incompressible flows with thermal convection. *International Journal for Numerical Methods in Fluids*, 17:271–289, 1993.

[5] H.-J. Ko and G. S. Dulikravich. A fully non-linear theory of electro-magneto-hydrodynamics. In D.A. Siginer and D.D. Kee, editors, *Symposium on Rheology and Fluid Mechanics of Nonlinear Materials.* ASME, Anaheim, CA, Nov. 1998 ASME FED-Vol. 246, MD-Vol. 81, pp. 173–182, 1998. Also to appear in Int. J. of Non-linear Mechanics, 2000.

[6] B.-N. Jiang and L.A. Povinelli. Optimal least-square finite element method for elliptic problems. *Comput. Methods Appl. Mech. Engrg.*, 102:199–212, 1993.

[7] S. S. Sazhin, M. Makhlouf, and T. Ishii. Solutions of magnetohydrodynamic problems based on a conventional computational fluid dynamics code. *International Journal for Numerical Methods in Fluids*, 21:433–442, 1995.

[8] N. B. Salah, A. Soulaimani, W. G. Habashi, and M. Fortin. A conservative stabilized finite element method for the magneto-hydrodynamic equations. *International Journal for Numerical Methods in Fluids*, 29:535–554, 1999.

[9] D. L. Marcum and N. P. Weatherhill. Unstructured grid generation using iterative point insertion and local reconnection. *AIAA Journal*, 33(9):1619–1625, September 1995.

[10] S. Balay, W. D. Gropp, L. C. McInnes, and B.F. Smith. PETSc 2.0 users manual. Technical Report ANL-95/11 - Revision 2.0.24, Argonne National Laboratory, 1999.

Table 1: Parameters for Poisuille-Hartmann flow test problem

Ht	10.0
Rm	6×10^{-7}
$L_0\,(m)$	1.0
$U_0\,(m\,s^{-1})$	0.6
$\eta\,(kg\,m^{-1}s^{-1})$	0.01
$B_0\,(T)$	1.0
$\mu\,(H\,m^{-1})$	1×10^{-6}
$\partial P/\partial x\,(Pa\,m^{-1})$	0.6
$\sigma\,(\Omega^{-1}m^{-1})$	1.0

Table 2: Physical parameters for channel problem

$\rho\,(kg\;m^{-2})$	1024.0
$L_0\,(m)$	1.0
$U_0\,(m\,s^{-1})$	6.0×10^{-4}
$\eta\,(kg\,m^{-1}s^{-1})$	0.001
$\mu\,(H\,m^{-1})$	1×10^{-6}
$\sigma\,(\Omega^{-1}m^{-1})$	4.5
$Cp\,(JKg^{-1}K^{-1})$	4184.0
$k_{fluid}\,(Wm^{-1}K^{-1})$	.5
$k_{solid}\,(Wm^{-1}K^{-1})$	10.0
$B_o\,(T)$	0.0-3.0

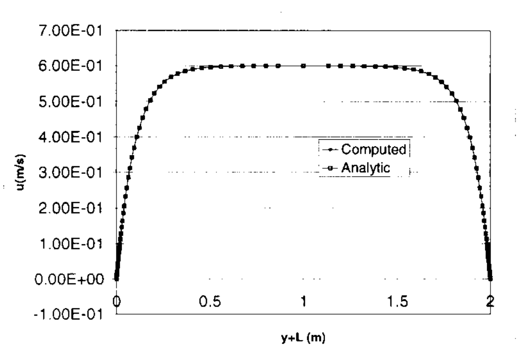

Figure 1: Computed and analytical values for velocity profile

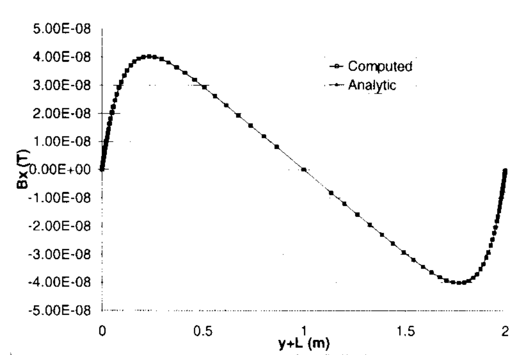

Figure 2: Computed and analytical values for induced magnetic field

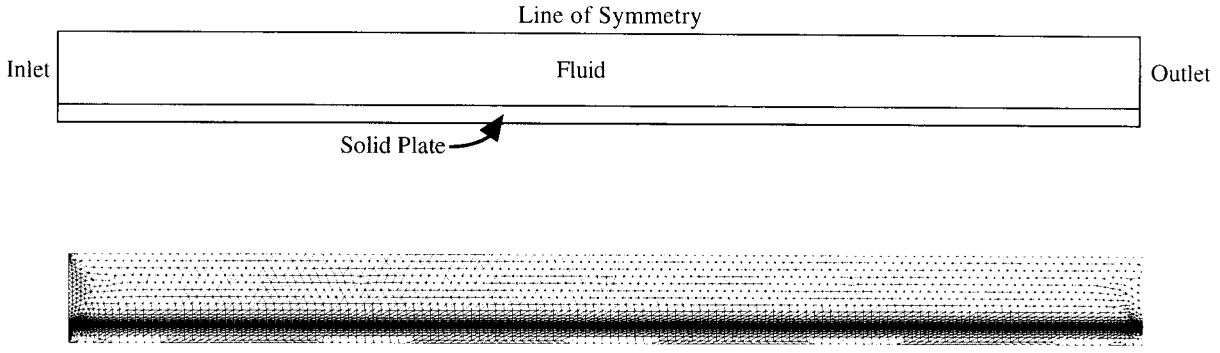

Figure 3: Computational domain and mesh for conjugate heat transfer problem

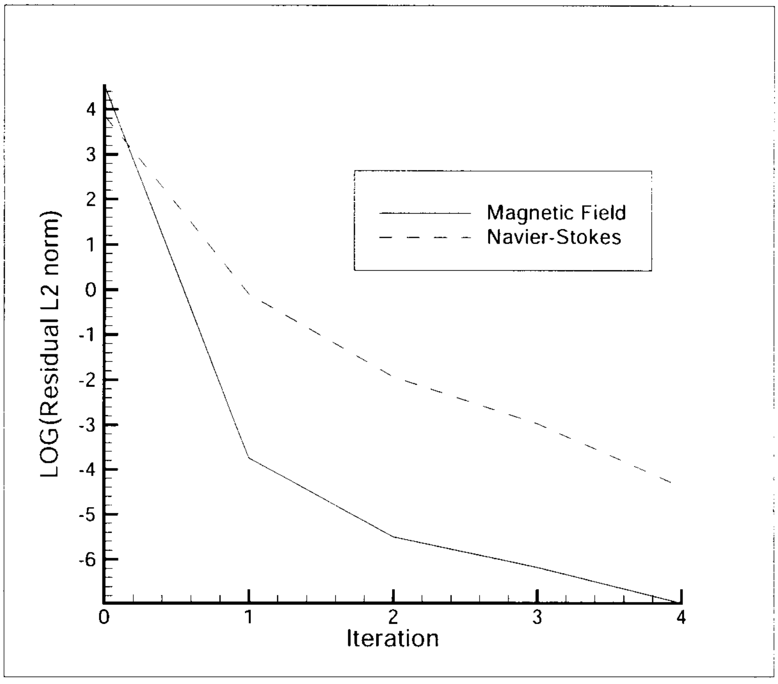

Figure 4: Convergence history for a typical MHD analysis

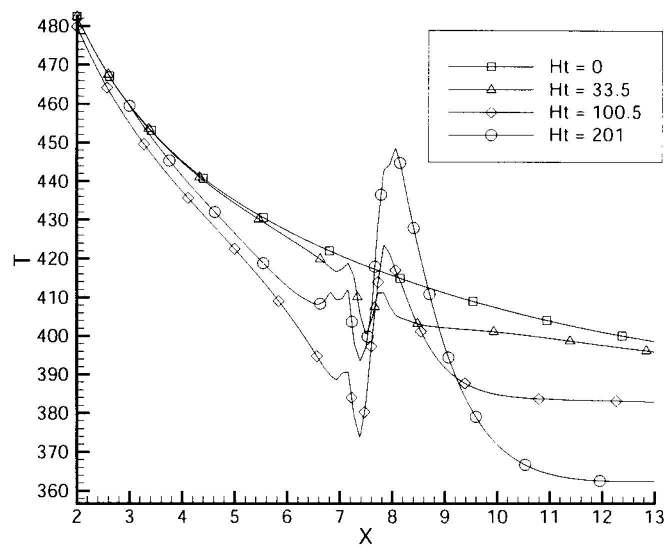

Figure 5: Temperature profile on fluid/solid interface

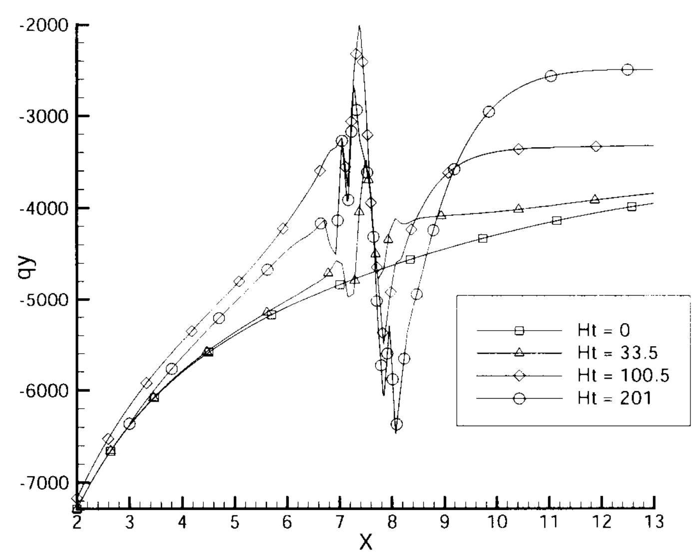

Figure 6: Heat flux profile on fluid/solid interface

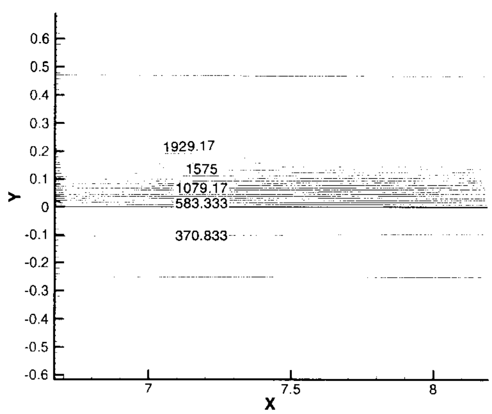

Figure 7: Temperature contours for $Ht = 0$

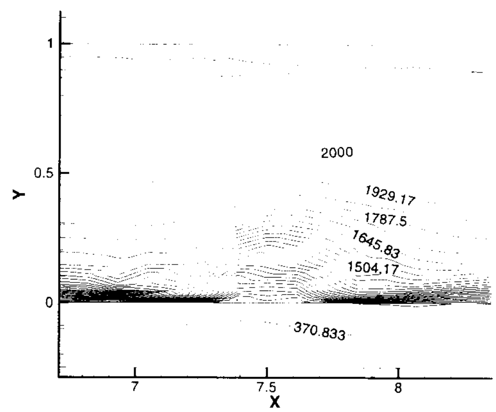

Figure 8: Temperature contours for $Ht = 335$

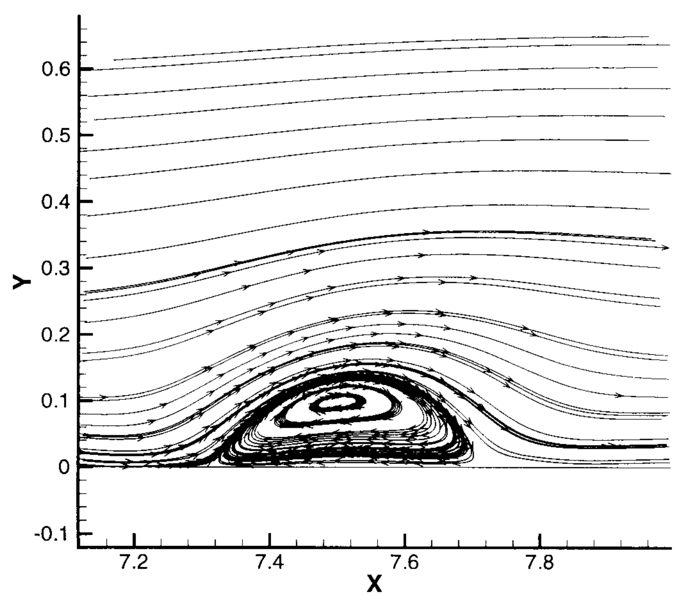

Figure 9: Vortex generated by applied magnetic field for $Ht = 102$

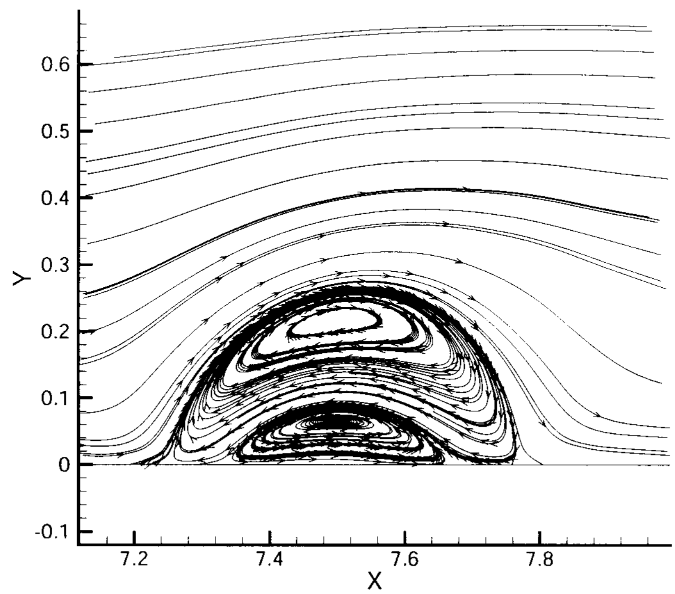

Figure 10: Vortex generated by applied magnetic field for $Ht = 201$

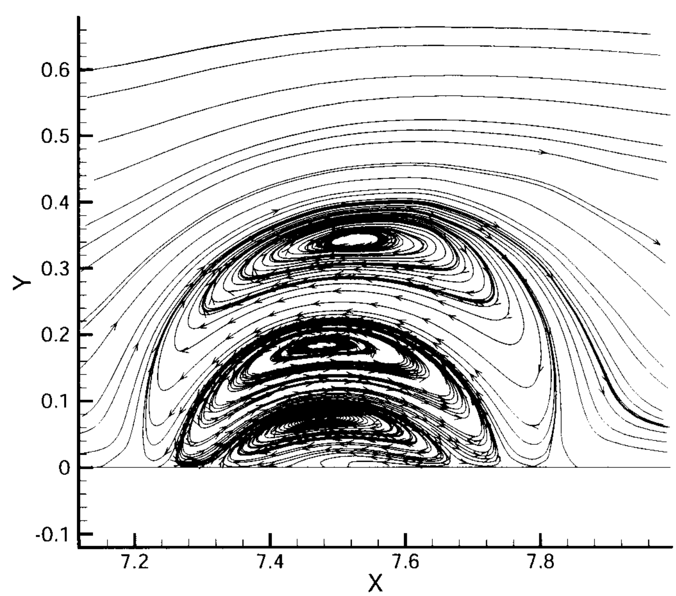

Figure 11: Vortex generated by applied magnetic field for $Ht = 335$

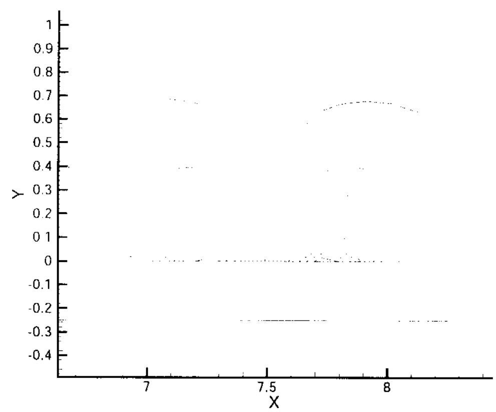

Figure 12: Contours of B_y for $Rm = 1E-9$

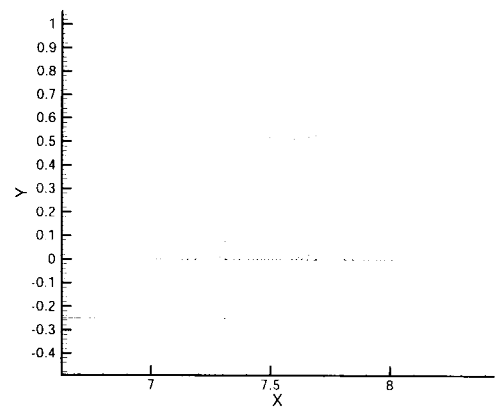

Figure 13: Contours of B_y for $Rm = 20$

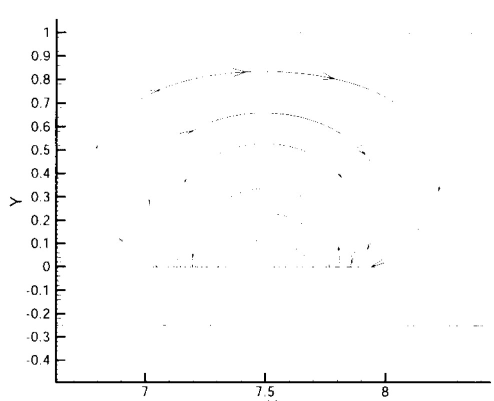

Figure 14: Magnetic field lines for $Rm = 2.7E-9$

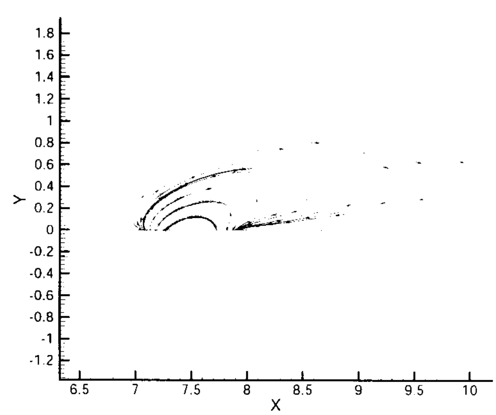

Figure 15: Magnetic field lines for $Rm = 20$